Progress in Applications of Prussian Blue Nanoparticles in Biomedicine

Zhiguo Qin, Yan Li, and Ning Gu*

Prussian blue nanoparticles (PBNPs) with favorable biocompatibility and unique properties have captured the attention of extensive biomedical researchers. A great progress is made in the application of PBNPs as therapy and diagnostics agents in biomedicine. This review begins with the recent synthetic strategies of PBNPs and the regulatory approaches for their size, shape, and uniformity. Then, according to the different properties of PBNPs, their application in biomedicine is summarized in detail. With modifiable features, PBNPs can be used as drug carriers to improve the therapeutic efficacy. Moreover, the exchangeable protons and adsorbability enable PBNPs to decontaminate the radioactive ions from the body. For biomedical imaging, photoacoustic and magnetic resonance imaging based on PBNPs are summarized, as well as the strategies to improve the diagnostic effectiveness. The applications related to the photothermal effects and nanoenzyme activities of PBNPs are described. The challenges and critical factors for the clinical translation of PBNPs as multifunctional theranostic agents are also discussed. Finally, the future prospects for the application of PBNPs are considered. The aim of this review is to provide a better understanding and key consideration for rational design of this increasingly important new paradigm of PBNPs as theranostics.

1. Introduction

Prussian blue (PB) is considered to be a promising coordination polymer for theranostics with the ideal formula of $Fe^{III}_4[Fe^{II}(CN)_6]_3 \cdot nH_2O$ in biomedical field.[1] A Berlin artist Diesbach first discovered PB in the early 18th century.[2] Keggin and Miles demonstrated the porous network cubic structure of PB using powder diffraction patterns in 1936,[3a] which was further confirmed via single crystal diffraction by Herren in 1980.[3b] The face-centered cubic unit cell of PB is composed of ferric, ferrous, and cyanide ions, and the space group is generally claimed as *Fm3m*. Ferric ions are connected to nitrogen atoms of cyanides, and ferrous ions are linked by carbon atoms of cyanides, which alternately coordinate to form a cubic unit cell.[4] The dimension of the unit cell is 10.2 Å and the average bond lengths of Fe(II)−, C−N, and Fe(III)−N≡C are 1.90, 1.13, and 2.03 Å, respectively.[5] An intervalent electron can transfer from iron(II) to iron(III) ions to generate absorption band near 700 nm, resulting in the widely used of PB as pigment in cultural objects.[6] PB can be divided into insoluble PB $(Fe^{III}_4[Fe^{II}(CN)_6]_3 \cdot nH_2O)$ and soluble PB $(KFe^{III}[Fe^{II}(CN)_6])$ on the basis of the structure (**Figure 1**).[7] For insoluble PB, water molecules will occupy the vacancies in the defective lattice and coordinate to iron ions to balance the charge, namely coordinative type, or enter into the inside cavities and uncoordinated to iron ions, namely zeolitic type. For soluble PB, alkali metal ions replace water molecules in the cavities to balance the charge. Due to the porous nature, PB can adsorb small molecules (ions or gas), which make it known as "chemical sponge" in the wide application of gas storage, environmental cleanup, drug delivery, and other fields.[8]

PB has been widely investigated in the fields of battery, sensor, and catalysis due to its excellent electrochemical and optical properties.[9] By regulating external potentials, the oxidation states of PB can be changed into Prussian white $(K_2Fe^{II}Fe^{II}(CN)_6)$, Berlin green $(K_{1/3}Fe(Fe^{III}(CN)_6)_{2/3}(Fe^{II}(CN)_6)_{1/3})$, and Prussian yellow $(Fe^{III}Fe^{III}(CN)_6)$ with different colors, respectively.[10] In the visible spectrum, PB and Berlin green have two absorption bands at 700 and 480 nm; Prussian white has no obvious band; Prussian yellow presents only a band at 420 nm. In addition, PB is considered as a peroxidase (POD) analog used for catalyzing the reduction of hydrogen peroxide.[11] It has also the ability to react in lower dosage. In view of this characteristic, PB has great potential application in biosensors.[12]

Although there have been lots of reports on PB, most of the studies are mainly focused on the utilization of battery electrodes and biosensors rather than theranostics of diseases. In fact, due to its specific ion-exchange, adsorption, and mechanical trapping properties, PB has been approved as an antidote for treatment of internal radioactive contamination with thallium and cesium by the U.S. Food and Drug Administration (FDA) in 2003. With the continuous innovation of nanoscience and nanotechnology, the nanocrystallization of traditional drugs has also inspired enormous research enthusiasm

Z. Qin, Dr. Y. Li, Prof. N. Gu
State Key Laboratory of Bioelectronics
Jiangsu Key Laboratory for Biomaterials and Devices
School of Biological Science and Medical Engineering
Southeast University
Nanjing 210009, China
E-mail: guning@seu.edu.cn

The ORCID identification number(s) for the author(s) of this article can be found under https://doi.org/10.1002/adhm.201800347.

ADVANCED
SCIENCE NEWS
www.advancedsciencenews.com

ADVANCED
HEALTHCARE
MATERIALS
www.advhealthmat.de

because of the unique superiorities of nanomaterials, such as the comparability to the biological molecule in size, high surface-to-volume ratio, easy surface modification and functionalization, fantastic solubility and stability, sustained drug release, and targeting behaviors.[13] Therefore, PB nanoparticles (PBNPs) with these advanced features are endowed with some novel applications in biomedical field. It has been proved that PBNPs can serve as theranostic agents based on their inherent bioactivities and imaging capabilities,[14] remove excess reactive oxygen species (ROS) from the body to treat the ROS-related diseases, and decompose the hydrogen peroxide into oxygen to overcome the hypoxia of solid tumors due to the nanoenzyme activities such as POD, catalase (CAT), and superoxide dismutase (SOD). The porous and surface-modifiable features endow PBNPs with the function to deliver active molecules to overcome the weaknesses of conventional drug, such as poor solubility, insufficient target specificity, and systemic toxicity. With these advanced features, the application of PBNPs in the diagnosis and therapy of diseases is a major stride forward for the development of PB-related nanodrugs.

In this review, we will concentrate on the progress of synthetic strategies of PBNPs to realize the controllable preparation of size, shape, and homogeneity so as to provide high-quality materials for future applications. We will also highlight the applications of PBNPs as drug carriers, antidote, contrast agents, photothermal converter, and nanoenzyme in biomedicine. Finally, we will discuss some key problems in the clinical translation of PBNPs as a theranostic agent to provide some references for further research (**Figure 2**).

## 2. Synthetic Strategies of PBNPs for Applications in Biomedicine

Generally, the preparative techniques of nanoparticles (NPs) have laid a foundation for its better application. With multiple unique properties, PBNPs have shown great potential in the diagnosis and treatment of diseases. In order to extend the application, improve the performance, and accelerate the clinical translation of PBNPs, the synthetic strategies have been widely exploited. Now, various methods have been utilized to prepare PBNPs, such as easy straightforward solution method, hydrothermal method, and hydrolysis method.[7,15] According to the synthetic strategies, the preparation methods of PBNPs can be divided into double-precursor synthesis and single-precursor synthesis (**Figure 3**), which both have been proved to be promising synthetic methods to fabricate PBNPs.[16]

In double-precursor synthesis process, equimolar amounts of Fe^{3+}/Fe^{2+} and $[Fe(CN)_6]^{4-}/[Fe(CN)_6]^{3-}$ solution are mixed directly to form PBNPs. For example, Uemura and Kitagawa successfully fabricated polyvinylpyrrolidone-protected PBNPs by mixing equimolar $FeCl_2$ and $K_3Fe(CN)_6$ solutions.[17] A variety of biocompatible polymers, such as chitosan (CS), polyethylenimine (PEI), oxalic acid, and poly(diallyldimethylammonium chloride) (PDDA), have been used as protective agents in previous studies.[18] The polymer protector can decrease surface energy, inhibit agglomeration, and increase the solubility of nanoparticles. Moreover, these polymers can also interact with drug molecules to facilitate the loading of drugs for the
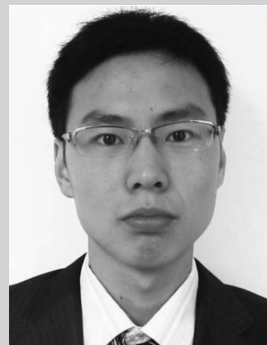
Zhiguo Qin received his B.S. from the China Pharmaceutical University in 2014. He is currently a Ph.D. candidate under the supervision of Prof. Ning Gu at the Department of Biological Science and Medical Engineering, Southeast University. His research includes the design, synthesis, and biomedical applications of Prussian blue nanoparticles.
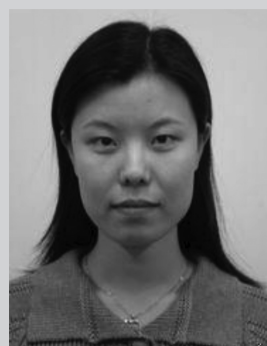
Yan Li received her Ph.D. degree from Tsinghua University in 2008. She is currently working at the Department of Biological Science and Medical Engineering, Southeast University. Her research includes the interactions between cells and biomaterials, biomedical applications of mesenchymal stem cells and the design and construction of drug delivery system, etc.

Ning Gu was born in 1964. He received his Ph.D. degree in biomedical engineering from the Department of Biomedical Engineering, Southeast University, Nanjing, China, in 1996. Currently he is a Changjiang Scholar Professor and NSFC Outstanding Young Investigator Fund Winner at Southeast University. He also serves as the president of Jiangsu Society of Biomedical Engineering, the director of the Research Center for Nanoscale Science and Technology of Southeast University, and the chief researcher of the Collaborative Innovation Center of Suzhou Nano-Science and Technology (2011 Program). His research interests include magnetic nanobiomaterials, nanobiology, medical imaging, advanced instrument development, etc.

collaborative treatment of diseases that will be described in detail in the "PBNPs for Drug Delivery" section. The advantage of this synthetic strategy is the shorter reaction time and no reducing agent. The single-precursor synthesis method was exploited first by Deng and co-workers in 1998.[19] Either
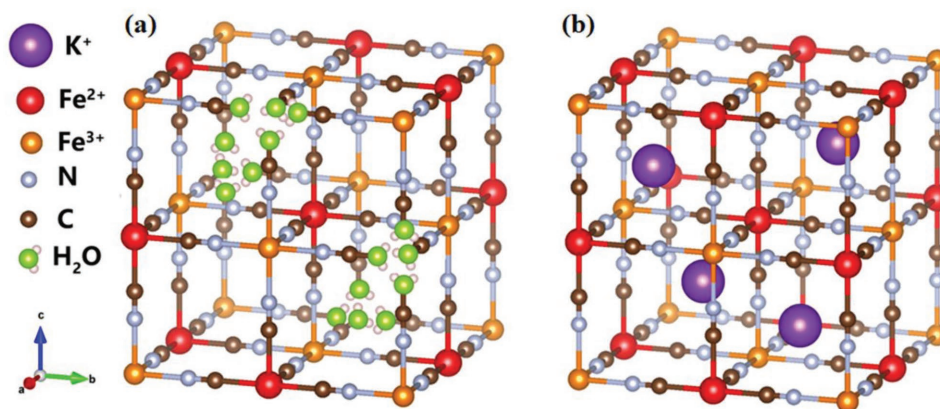
ADVANCED
SCIENCE NEWS
www.advancedsciencenews.com

ADVANCED
HEALTHCARE
MATERIALS
www.advhealthmat.de

Figure 1. Scheme of unit cell of a) insoluble $\{Fe^{III}_4 [Fe^{II}(CN)_6]_3 \cdot xH_2O\}$, and b) soluble $\{KFe^{III}[Fe^{II}(CN)_6]\}$.

$K_3[Fe(CN)_6]$ or $K_4[Fe(CN)_6]$ is commonly used as a precursor, which can slowly release Fe^{3+} or Fe^{2+}, reduced, or oxidized into Fe^{2+} or Fe^{3+} in acidic solution.[20] The formed Fe ions can immediately react with the precursor to generate PBNPs. The superiority of this synthetic strategy is able to gain preferable uniformity of nanoparticles with simple operations due to the slow reaction processes.

However, both synthetic strategies still need further optimization to satisfy with the application of PBNPs for diagnosis and treatment of diseases. As for double-precursor synthesis,

Figure 2. Different applications of PBNPs in biomedicine, namely, imaging, therapy, drug delivery, and some key factors for clinical translation.

the dispersion uniformity, reproducibility, and morphological regulation need to be further improved. The single-precursor preparation process takes a long time, and a trace of hydrogen cyanide can be produced in the process of reaction that may hinder the application of this method in scale production. In fact, the size, morphology, and uniformity have an appreciable impact to the properties of PBNPs,[21] which are closely related to the synthetic conditions and procedures. Thus, to acquire the high-quality PBNPs for efficient and safe application in biomedicine, there is still a need to develop a size-, shape-, and homogeneity controllable synthesis method with simple procedures.

To precisely regulate the size and morphology of PBNPs, the various synthesis conditions have been investigated. Hu et al. demonstrated that polyvinylpyrrolidone (PVP) could serve as a reducing agent to prepare PBNPs using single-source precursor in acidic solution.[22] They fabricated three different sizes (20, 100, and 200 nm) of PBNPs by systematically adjusting the concentration of PVP, $K_3[Fe(CN)_6]$, and hydrochloric acid in the reaction mixture. The growth process of PBNPs was demonstrated to be a nonclassical crystallization. Shen et al. discovered that the morphology of PBNPs could be tuned by controlling the reaction temperature.[23] When the reaction temperature was under 130 °C, the shape of PBNPs was nanocubes; at 140 °C, both nanocubes and nanospheres existed; and between 150 and 170 °C, only nanosphere could be formed. PB microframes could be produced by adding electron donor ascorbic acid into the reaction solution. Hence, the growth of the PBNPs could be intensely influenced by the types of reductants. In addition, polysaccharide,[24] grapheme oxide,[25] and polyaniline[26] have also been used as electron donors for the preparation of PBNPs.

Apart from temperature and reductants, the concentration of acid also played a crucial
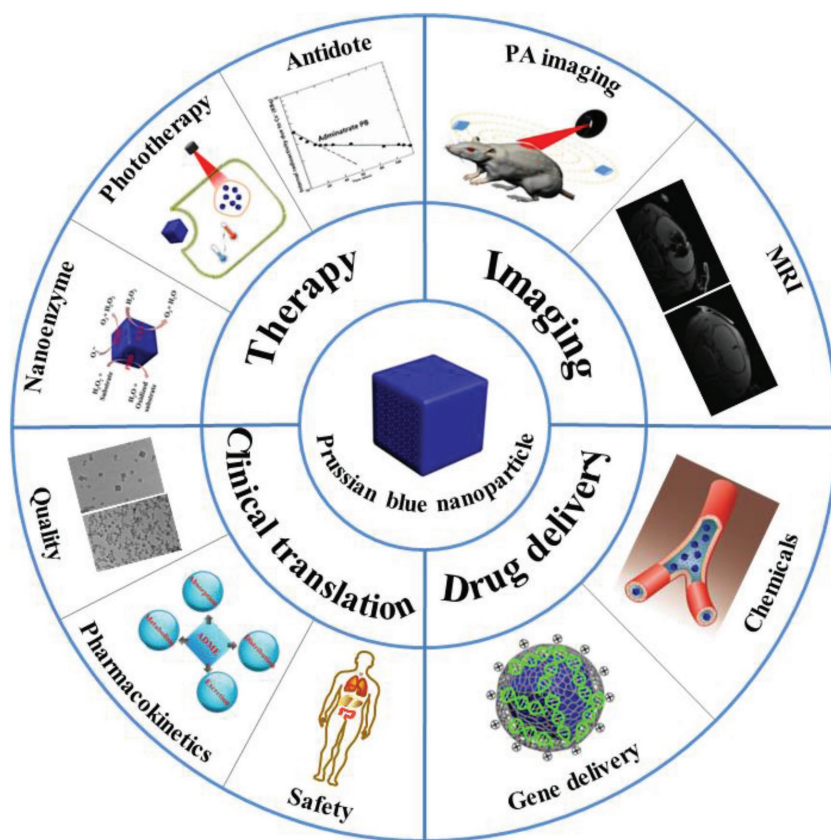
**ADVANCED
SCIENCE NEWS**
www.advancedsciencenews.com

**ADVANCED
HEALTHCARE
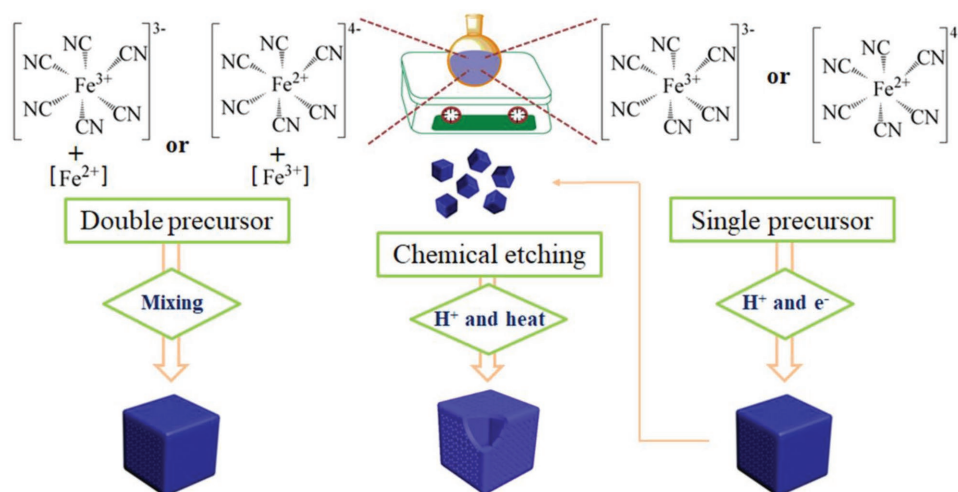MATERIALS**
www.advhealthmat.de

Figure 3. Illustration of the synthetic processes of PBNPs.

role on the morphology of PBNPs during the single-precursor synthesis. By increasing the acidity and temperature of reaction solution, solid PBNPs can be selectively etched into hollow structure when a capping polymer or surfactant is used to protect the surface of PBNPs. The prepared hollow PBNPs can be employed as a drug carrier with supernal drug loading capacity. The details will be discussed in the "PBNPs for Drug Delivery" section. Hu et al. synthesized an interior hollow-structured PBNP by controlled chemical etching in a higher concentration of hydrochloric acid solution at 140 °C for 4 h,[27] using PVP as the capping agent to protect the surface of PB mesocrystals. Etching agent (H^+) could permeate into the PB mesocrystals via the defects resulting in a higher concentration in the inner. Thus, the etching rate in the center was faster than that on the surface of PBNPs, leading to the formation of hollow cavity. In another work, they further reported that shell-in-shell hollow PBNPs were prepared by controlling the rates of crystal growth and etching.[28] Lee and Huh verified that by adjusting the concentration of HNO_3 in the etching process, PBNPs with various shapes could be synthesized, such as truncated cubes, octahedron, and star-like hexapod.[29] They also perceived that the {111} planes of PB nanocubes would be etched preferentially in the preparation process.

To further improve uniformity of nanoparticles in the size and shape, several synthetic strategies have been developed. Microemulsion is an effective technique for this purpose by controlling the nucleation and crystal growth of PBNPs.[30] Vaucher et al. performed a reverse microemulsion (water-in-oil) using sodium bis(2-ethylhexyl) sulfosuccinate (AOT) as the surfactant to prepare PBNPs.[31] They observed that $[Fe(C_2O_4)_3]^{3-}$ could slowly generate Fe^{2+} under daylight, which subsequently coordinated with $[Fe(CN)_6]^{3-}$ to realize the control of nanoparticles growth in the water phase. In another work, Wang and co-workers explored a miniemulsion periphery polymerization (MEPP) method to prepare PB nanoshells and nanoboxes by changing the experimental conditions.[32] Furthermore, Cornelissen and co-workers discovered that cowpea chlorotic mottle virus (CCMV) without RNA could be used as a nanoreactor for the preparation of monodispersed PBNPs

with favorable dispersity and a diameter of 18 nm. Due to the ability of assembling/disassembling in different pH solutions, CCMV capsid can encapsulate $[Fe(C_2O_4)_3]^{3-}$ and $[Fe(CN)_6]^{3-}$ together. Exposed to light reagents, the reaction between the two reagents was activated.[33] In addition to CCMV, apoferritin, mesoporous silica, liposome, and porous alumina have also been used as template to fabricate PBNPs in recent years.[34]

Recently, the outfield-assisted method is supposed to be another novel synthesis technique that can effectively improve the dispersion uniformity by influencing the formation, nucleation rate, and crystallization of PBNPs during the preparation. Wu et al. developed a sonochemical synthesis to prepare PBNPs with uniform size distribution utilizing precursor $K_4[Fe(CN)_6]$ in an acidic solution.[35] Our group has developed an alternating magnetic field–assisted synthesis method to prepare magnetic nanoparticles via magnetic thermal effect.[36] PBNPs can also be synthesized by this method due to their inherent magnetism. Compared to traditional external heating approaches, this synthesis technique can realize homogeneous heating for reaction system to generate a high-quality PBNPs.

3. PBNPs for Drug Delivery

PBNPs is a novel and potential drug delivery system due to their inherent features of stability in blood, biocompatibility, biodegradability, low cytotoxicity, low cost, easy preparation, tunable morphology, and controllable size, which can be applied to satisfy the various requirements for different drug delivery, such as high drug loading efficiency and target specificity (**Figure 4**). There have been some advances in drug delivery systems based on PBNPs in the last few decades, which have generated significant breakthroughs in cancer and infection therapy.[37] PBNPs have demonstrated the capacities to enhance therapeutic efficacy, reduce systemic toxicity, and deliver theranostic agents to organs, tissues, and cells.

As for the drug carrier, there are two strategies to address the requirements for drug loading of PBNPs. One method is to fabricate the hollow mesoporous PBNPs to improve the surface
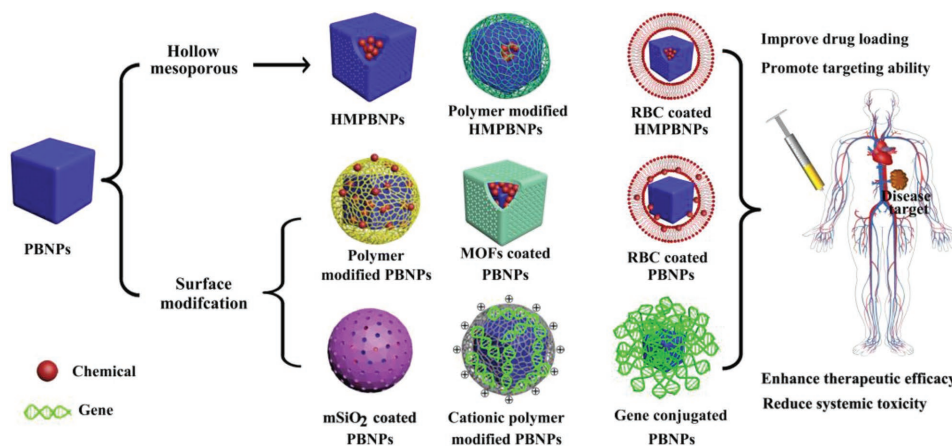
Figure 4. The commonly used drug delivery nanoplatforms based on PBNPs vary from hollow mesoporous PBNPs (HMPBNPs), such as polymer-modified and RBC-coated HMPBNPs, to surface modification PBNPs like polymer-modified, MOF-coated, RBC-coated, mSiO₂-coated, cationic polymer-modified and gene-conjugated PBNPs.

area and the drug loading capacity. For example, Chen et al. prepared a near infrared (NIR) light responsive co-delivery system (PCM+drugs)@HMPBNPs based on hollow mesoporous PBNPs (HMPBNPs) and a phase change material; the nanoparticles revealed near "zero release" of both hydrophobic camptothecin and hydrophilic doxorubicin (DOX) hydrochloride, and demonstrated synergistic photothermal-chemo effects against HeLa cancer cells.[38] Cisplatin was also successfully loaded in HMPBNPs to deliver into cancer cells in vitro.[39]

Unfortunately, bare HMPBNPs without surface modification tend to be removed by immune system and prematurely leak drug before reaching the target sites, thus, leading to low therapeutic efficacy and high toxic side effects. It was reported that the surface modification of hyaluronic acid grafting polyethylene endowed the 10-hydroxycamptothecin-loaded HMPBNPs with enhanced colloidal stability, prolonged blood circulation time, and tumor targeting capacity.[40] However, polyethylene can produce anti-immunoglobulin M antibodies to induce immune response.[41] To improve the immune evading capability, the red blood cell (RBC) membrane–coated HMPBNPs encapsulating DOX was fabricated with a drug loading of 130%. Both in vitro and in vivo experiments demonstrated that this system presented low toxicity and excellent synergistic photothermal chemotherapy of cancer.[42]

Another approach to improve the drug loading capacity of PBNPs is to modify their surface with organic or inorganic materials, other metal–organic frameworks (MOFs) and cell membrane. Chen et al. reported lipid–poly(ethylene glycol) (PEG) conjugation–modified PBNPs to encapsulate doxorubicin via hydrophobic interactions.[43] DOX-conjugated gelatin was also used to stabilize the PBNPs for combined photothermal chemotherapy.[44] For inorganic materials, Su et al. revealed that the PB@mSiO₂–PEG/DOX nanoplatform exhibited good biocompatibility, excellent pH-responsive drug release, and enhanced synergistic photothermal chemotherapy for breast cancer.[45] MOFs have been widely investigated to decorate the PBNPs to construct "dual MOFs" for drug delivery, such as ZIF-8 and MIL-100(Fe).[46] To increase the loading capacity of doxorubicin and prolong the circulation time in vivo, a nanocarrier,

named PBMn–DOX@RBC, was fabricated by coating a RBC membrane onto PB/MnO₂ (PBMn) nanoparticles.[47]

Without appropriate modifications, exogenous nucleic acids tend to degrade by extracellular deoxyribonucleases and impede cellular uptake.[48] PBNPs have also promising nuclease-resistance strategies as well as cargo roles, which can be considered as a counter part for nucleic acids. Wang et al. prepared the DNA–PBNP gene delivery system by grafting DNA onto 11-mercaptoundecanoic acid (MUA) chemically modified PBNPs.[49] The results demonstrated that the PBNPs indeed fulfill internalization and homogeneous distribution of the DNA in human prostate carcinoma 22Rv1 cells and enhanced the cancer cell-killing ability. Li et al. reported that MBs@CS/PB/DNA demonstrated outstanding ultrasound (US) imaging capability and enhanced gene transfection efficiency.[50]

Both of these two loading strategies have their merits. The process to prepare drug-loaded HMPBNPs is simple and adjustable, but not industrially feasible. Surface-modified PBNPs present the advantages of high drug loading, enhanced stability, good biocompatibility, and multifunction integration. Nevertheless, the reproducibility and controllability are not ideal enough.

4. Treatment of Radiocesium and Thallium Poisoning

PBNPs have shown several biological activities for the treatment of diseases. Both the porous structure and internal exchangeable ions endow PBNPs with the function to accelerate the removal of radiocesium and thallium ions from the body. The insoluble PB (trade name Radiogardase) has been approved to treat patients with internal contamination of radioactive cesium (Cs⁺) and/or radioactive or nonradioactive thallium (Tl⁺) by FDA, which is the only formulation currently available to reduce the biological half-life of these radioactive ions in clinical medicine. The proton exchange, surface adsorption, and mechanical trapping within the crystal structure are the primary mechanisms for decontamination. The

adsorption of Cs^+ and Tl^+ is a highly selective process with a pseudosecond-order kinetic model.[51] In addition, the structure type of PB also influences the clearance capacity for Cs^+ and Tl^+. Ishizaki et al. verified that the therapeutic efficacy of soluble PB was lower than that of insoluble PB.[52] Vacant sites, occupied by the coordination water molecules, are very common in the structure of insoluble PB. The Cs^+ was preferably adsorbed to the defect sites of PB crystal by ion exchange with the coordination water. Therefore, a higher-performance adsorbent could be obtained by synthesizing a PB with more water molecules.

However, it has been demonstrated that the external surface of PB crystal is the only bonding site for Cs^+ and Tl^+ because of the minuscule intracrystalline diffusion coefficient (less than 3.3×10^{-22} m^2 s^{-1}).[53] The Cs^+ can penetrate only 1–2 units of the crystalline lattice after 2 weeks at room temperature.[54] These factors significantly affect the adsorption rate and prolong the time of adsorption equilibrium. It is of great significance to develop uniform PBNPs with large specific surface area. Lavaud et al. revealed that nanosized PB possessed a faster kinetics and a larger capacity than the commercially available bulk PB for Cs^+ elimination in vivo.[55] In another study, Koshiyama et al. verified that discrete PBNPs, prepared within liposome, exhibited higher adsorption efficiencies than aggregated PBNPs, because the surface area was a crucial factor to improve adsorption capacity.[56]

For clinical application, PBNPs should also possess good biocompatibility and minor side effects. Qian et al. prepared poly(ethyleneglycol) (PEG)-modified PBNPs with high biocompatibility to directly eliminate Cs^+ from human blood.[57] Sandal et al. gelated sodium alginate (Alg) with calcium ions to encapsulate PB to develop an intestinal release delivery system, which increased the removing efficacy of Cs^+ and Tl^+ at a lower dose with minimum side effects.[58]

5. Biomedical Imaging Based on PBNPs

Nanoparticle-based contrast enhancement agents have been extensively researched to improve the quality of imaging.[59] PBNPs have been exploited as contrast agents for photoacoustic imaging and magnetic resonance imaging due to their unique feature and structure.[60] PBNPs with good biocompatibility and safety have attracted extensive research interests in biomedical diagnosis.

5.1. Photoacoustic Imaging

Photoacoustic tomography is a promising noninvasive imaging technique that possesses high penetration depth (several centimeters), remarkable temporal (100 ms) and spatial resolution (50–150 µm). Image resolution depends on the ultrasound wave diffraction, the detectors, and the photoacoustic contrast agent. Nanoscaled NIR absorbers, presenting rarely weak optical absorption of background tissue in this region, are effective photoacoustic contrast agents to improve signal-to-noise ratio (SNR).[61] With high molar extinction coefficient, PBNPs have been developed as an emerging contrast agent for photoacoustic imaging first by Liang et al. in 2013.[62] Compared with other arisen nanoscaled NIR absorbers (such as polypyrrole (PPy) NPs, gold NPs, and CuS NPs), PBNPs have displayed favorable biocompatibility, higher photothermal conversion efficiency, photostability, and easy size controllability. The photoacoustic signal was significantly enhanced under the maximum thickness of 4.3 cm in chicken breast tissues using citrate-coated PBNPs as a contrast agent in vitro. The in vivo experiments demonstrated that a clear brain vasculature image was acquired and remained from 15 to 60 min after intravenous administration of PBNPs, suggesting a prolonged blood circulation time. PBNPs showed no apparent acute toxicity to vital organs within 30 days by histological section. Au nanoparticles coated with PBNPs were also constructed to increase the photostability and applied for CT/photoacoustic bimodal imaging for cancer diagnosis.[63]

As a photoacoustic imaging contrast agent, PBNPs have been exploited as stem cell tracer in vivo due to their small size, unexceptionable biocompatibility, and readily internalized by cell. With this technique, the stem cell can be real-time monitored and dynamically visualized in the process of migration and differentiation. Kim et al. demonstrated that the stem cells could be labeled efficiently with PBNPs without any changes on cell viability or proliferation.[64] The strong photoacoustic signal was observed over a period of 14 days in living mice after intravenous administration of PBNPs. The cell concentration could also be quantified by calculating the photoacoustic signal strength. In another study, Li et al. utilized PBNPs to label bone mesenchymal stem cells (BMSCs) to image the traumatic brain injury and monitor recovery process.[65] The results indicated that BMSCs could overcome blood–brain barrier, home to damaged area and facilitate the recovery.

To further improve the efficiency of photoacoustic imaging, Cai et al. integrated Gd^{3+} into PB nanocrystals lattice site, which tuned the NIR absorption peak of PBNPs from 710 to 910 nm with higher penetration depth in tissue.[66] After Fe^{3+} being replaced by Gd^{3+} in PB nanocrystals, the electronic transition, electron density, charge carriers, and orbital energies of the cyanide bonds could be changed to generate the shift of maximum absorption.

5.2. Magnetic Resonance Imaging

In general, magnetic resonance imaging (MRI) contrast agents mainly include T_1-weighted agents with positive image effect (bright spots) and T_2-weighted agents with negative image effect (dark spots). Because it is difficult to recognize the dark region from the background, T_2-weighted imaging is not satisfied.[67] PBNPs with a unique crystal structure had been first developed as a T_1-weighted agent by Shokouhimehr et al. in 2010.[68] The mechanism of PB for magnetic resonance imaging is different from a conventional super-paramagnetic iron oxide nanoparticle (SPIO) system, which creates magnetic resonance imaging only via the outer-sphere relaxation mechanism. According to the Solomon–Bloembergen–Morgan (SBM) theory, the contrast efficiency may be ascribed to the inner-sphere longitudinal relaxation arising from the coordinative water protons with Fe^{3+} ($S = 5/2$) in insoluble PB. With

**ADVANCED
SCIENCE NEWS**
www.advancedsciencenews.com

**ADVANCED
HEALTHCARE
MATERIALS**
www.advhealthmat.de

the increase of coordinative water protons, the better contrast efficiency could be acquired.

Shokouhimehr et al. demonstrated that the value of longitudinal (r_1) and transverse (r_2) relaxivities of PBNPs were 0.079 and 0.488 mM^{-1} s^{-1} at 1.5 T, respectively.[69] Compared to the commercial MRI contrast agents, such as Gd^{3+}-based Pro-Hance (r_1 = 3.5 mM^{-1} s^{-1}), the value of PBNPs was relatively weaker. Nevertheless, PBNPs still received close attention in the biomedical imaging because of their outstanding stability with almost no iron ions and cyanide release in physiological, low cytotoxicity, excellent biocompatibility, and multiple functions. Liu et al. employed NaDyF4:50%Lu to modify the surface of PBNPs to realize multifunctional imaging for cancer diagnosis and imaging-guided therapy.[70]

The way to increase the longitudinal relaxivity of PBNPs has been studied by several groups recently. An effective strategy is to dope high-spin transition metal ions to PB nanocrystal structure. Cai et al. claimed that the value of r_1 could be tremendously increased from 0.14 to 7.43 mM^{-1} s^{-1} by adding Mn^{2+} (S = 5/2) to the outer surface and inner mesoporous channels of HMPBNPs.[71] They also revealed that the biosafety and therapeutic efficiency were well-satisfied. In another work, Dumont et al. demonstrated that the MRI signal intensity was increased to nine times compared with the clinical preparations by doping Gd^{3+} (S = 7/2) into the interstices of PB lattice. The in vitro studies showed that the nanocomposites could precisely visualize eosinophilic cells via MRI.[72]

5.3. Multimodal Imaging

Although single-modal imaging has been extensively used in the clinical diagnosis of diseases, it still possesses inextricable shortages. Combination of two or more imaging modalities can achieve complementary merits and more accurate imaging for pathological tissue.[73] PBNPs with multiple imaging modes and drug loading capacity have been explored for multimodal imaging-guided therapy, and their excellent performance has also been verified.[74] Tian et al. demonstrated that the combination of magnetic resonance (T_1) and photoacoustic imaging based on PBNPs could monitor the tumor regions and the accumulations of the loaded anticancer drug doxorubicin for theranostic of triple negative breast cancer without obvious side effect from histopathological analysis.[75] In another work, Zhang et al. prepared a nanotheranostic agent for photoacoustic and ultrasound dual-mode imaging based on doxorubicin- and perfluorohexane-encapsulated HMPBNPs.[76] The constructed nanocomposite with higher cavitation effect could enhance the therapeutic efficacy of high-intensity focused ultrasound and monitor the treatment procedure for cancer. Besides, a trimodal imaging-guided chemo-photothermal tumor therapy strategy based on hollow PBNPs has been explored by Li et al.[77] The combination of magnetic resonance imaging (T_1), photoacoustic imaging, and infrared thermal imaging could clearly indicate the tumor site.

PBNPs can also combine with other contrast agents to form multifunctional core@shell heterostructures nanotheranostic platforms. Yang et al. fabricated a Fe$_3$O$_4$@PB nanoparticle via in situ growth of PB shell on the surface of Fe$_3$O$_4$ nanoparticle, followed by coupling with CuInS$_2$–ZnS quantum dots (QDs),

which served as an NIR fluorescent imaging agent.[78] The bimodal imaging of magnetic resonance (T_2) and NIR fluorescence imaging could be further used to evaluate the therapeutic efficacy. Dou et al. designed PB@Au core–shell nanoparticles with magnetic resonance and computed tomography imaging-guided treatment for cancer.[79] The results showed that the tumor growth was inhibited without obvious systemic toxicity. Additionally, Peng et al. coated carbon dots (CDs) on the surface of PBNPs by a microwave-assisted synthesis method to construct a fluorescence imaging-guided therapy nanoplatform.[80]

6. PBNPs in Therapeutic Hyperthermia

PBNPs can efficiently convert NIR light into thermal energy to elevate the temperature because of the charge transfer between Fe^{3+} and Fe^{2+} via cyanide ion. Moreover, the molar extinction coefficient of PBNPs (1.09×10^9 M^{-1} cm^{-1} at 808 nm) is significantly higher than that of conventional photothermal agents such as carbon nanotubes (7.9×10^6 M^{-1} cm^{-1} at 808 nm) and Cu$_{2-x}$Se (7.7×10^7 M^{-1} cm^{-1} at 808 nm), although slightly lower than that of Au nanorods (5.24×10^9 M^{-1} cm^{-1} at 808 nm). PBNPs possess a high light-to-heat conversion efficiency. In addition, the photostability and dispersible of PBNPs in both water and biological mimic environments are fantastic. For these reasons, PBNPs have widely been developed as photothermal ablation agent for treatment of disease. Fu et al. operated PBNPs to treat cancer under irradiation at 808 nm laser for the first time.[81] According to the study, the temperature could be increased to a critical value (43 °C) for treating cancer at a low PBNP concentration of 500 ppm when exposed to 808 nm laser within 3 min. The cytotoxicity evaluation revealed that cell viability was decreased to 10% after treatment by photothermal ablation.

The photothermal therapeutic efficacy may depend on the concentration, size, morphology, chemical composition, and surface modification of nanoparticles.[82] The external factors such as the laser power and irradiation time can also influence the efficiency. Indeed, Zhu et al. highlighted that the photothermal conversion performance was increased by doping Mn^{2+} into PBNPs compared to the nondoped PBNPs.[83] Coating polyethylene glycol onto the surface of PBNPs could improve the stability under the physiological conditions, promote the accumulations in the tumor, and then increase the photothermal therapeutic efficacy. Functional molecules such as the antibody, peptides, and gene can also be conjugated on the surface of PBNPs to enhance the photothermal cytotoxicity. Li et al. demonstrated that glypican-3 antibody functionalized PBNPs could be selectively transported to tumor tissue and improve the photothermal therapeutic efficacy.[84]

PBNP-based photothermal effect can also be used for eradication of bacteria. Maaoui et al. reported that virulent strains of *Escherichia coli* and methicillin-resistant *Staphylococcus aureus* could be effectively ablated by PVP-coated PBNPs via photothermal therapy at 980 nm which exhibiting deeper tissue penetration.[85] Moreover, the specifically ablation of bacteria over mammalian cells could be acquired by adjusting the concentration of nanoparticles. This approach showed great potential in the treatment of diseases caused by drug-resistant bacteria.

The heat produced by the photothermal conversion of PBNPs can not only cure disease but also cause the liquid–gas phase
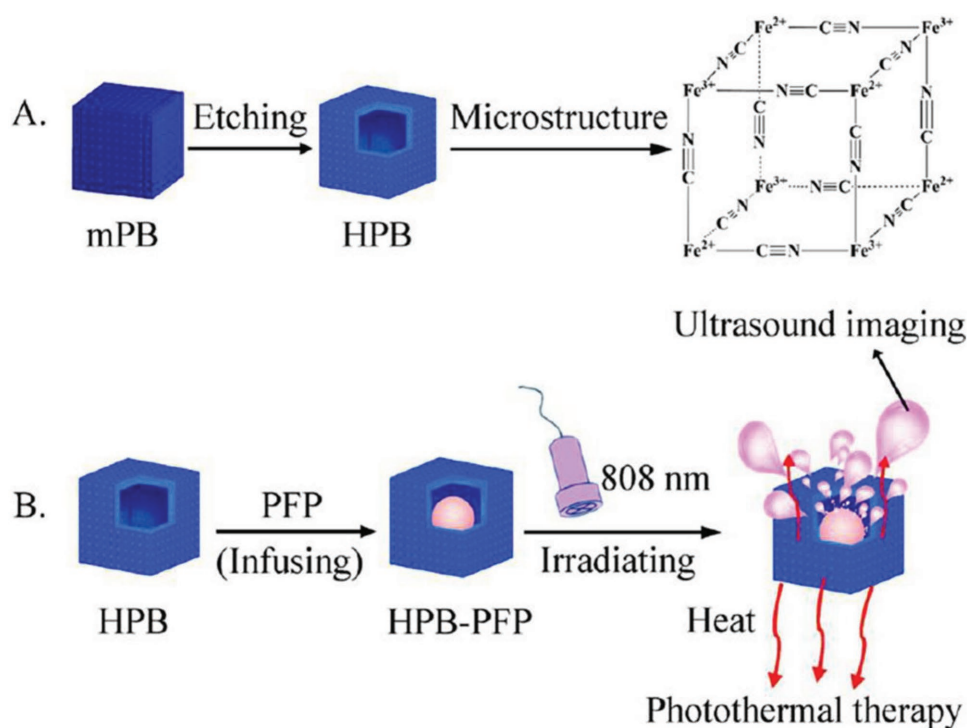
ADVANCED
SCIENCE NEWS
www.advancedsciencenews.com

ADVANCED
HEALTHCARE
MATERIALS
www.advhealthmat.de

Figure 5. a) Schematic illustration of the preparation process of hollow mesoporous Prussian blue (HPB) and its microstructure. b) Schematic illustration of HPB–n-perfluoropentane (PFP) formation and US-guided PTT upon laser irradiation. Reproduced with permission.[87] Copyright 2015, American Chemical Society.

change and bubble formation of low-boiling-point materials. The generated gas-filled bubbles as acoustic contrast agents with the ability to reflect and refract ultrasound waves can improve the sensitivity of US imaging to obtain a distinct image of tissues.[86] Jia et al. exploited a perfluoropentane-encapsulated hollow PBNP as a probe for ultrasound imaging.[87] The hollow PBNPs could convert NIR light energy into heat to gasify the volatile liquid perfluoropentane to create bubbles, which could strengthen the ultrasound imaging in vitro and in vivo. They further verified that this nanoplatform could be used for ultrasound imaging-guided photothermal therapy (PTT) of cancer (**Figure 5**). In another work, Cai et al. entrapped perfluoropentane and doxorubicin into hollow PBNPs together to construct a smart nanoplatform for ultrasound/photoacoustic dual mode imaging-guided thermal chemosynergistic therapy.[88]

7. Nanoenzyme for Theranostic

PBNPs have been extensively used as POD mimetic in biomedicine.[89] Very recently, we further found that PBNPs also possessed CAT- and SOD-like activities.[90] Similar to the natural enzymes, the catalytic kinetic behavior of PBNPs nanoenzyme followed the Michaelis–Menten equation and depended on the concentration, temperature, and pH. The K_{cat} value (1.16×10^5) of PBNPs was nearly an order of magnitude higher than that of Fe_3O_4 nanoparticles (3.02×10^4). PBNPs with different forms (such as reduced Prussian white, oxidized Berlin green, and Prussian yellow) have diverse redox potentials, which affect the catalytic reaction mechanisms. Without the Fenton reaction, PBNP

nanoenzyme could effectively eliminate ROS such as hydrogen peroxide, hydroxyl radicals, and superoxide radicals, which could cause several pathological processes. With these unique performances, PBNPs had been used as anti-inflammatory agent to protect cells from ROS damage and achieved a great therapeutic effect in mice inflammation models induced by lipoproteins.

PBNPs with CAT-like activity can catalyze the decomposition of hydrogen peroxide into oxygen under the neutral condition. The generated oxygen can relieve the tumor hypoxia situation, which plays an important role in tumor growth and metastasis. In view of these facts, several groups have developed multiple nanoplatforms based on PBNPs to improve the diagnosis and treatment efficacy for cancer. Zhou et al. designed a tumor-targeted redox-responsive nanocomposite for starvation and photothermal therapy of tumors.[91] Porous hollow PBNPs were not only used as carriers for glucose oxidase (GOx) to catalyze the oxidation of glucose to starve tumor cell under oxygen-adequate conditions, but also utilized to decompose hydrogen peroxide into oxygen molecules to further enhance glucose depletion. Moreover, this system could downregulate the expression of heat shock proteins (HSPs) to improve the photothermal therapy (**Figure 6**). In another work, Peng et al. prepared a PBMn nanoparticle coated by erythrocyte membrane to carry doxorubicin and prolong the circulation time in vivo.[47] The catalytic action of PBMn could generate oxygen to accelerate the release of doxorubicin by disrupting the erythrocyte membrane and relieve the hypoxic tumor to increase the therapeutic effect.

Interestingly, the oxygen produced by PBNPs' catalysis also has some applications in the diagnosis of diseases. Our group
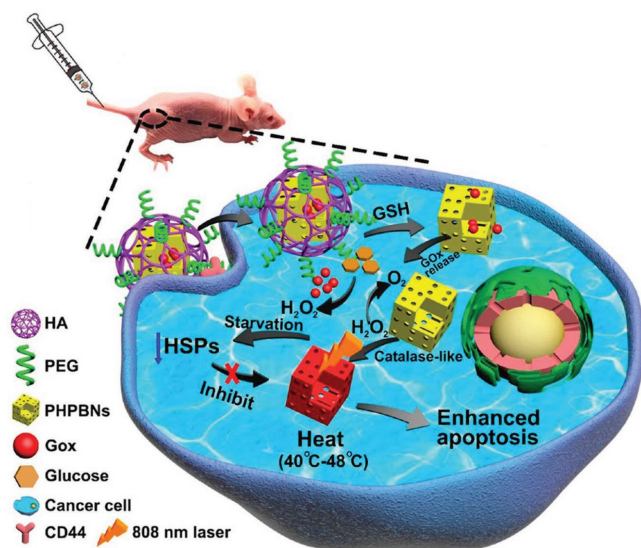
Figure 6. Illustration of GOx-induced starvation therapy based the PHPBN-mediated tumor reoxygenation. Reproduced with permission.[91] Copyright 2018, American Chemical Society.

developed an oxygen bubble nanogenerator for ultrasound imaging in the presence of H_2O_2, which could be catalyzed into oxygen molecules by PBNPs under neutral condition.[92] When the oxygen concentration reached the supersaturation in tissues, the bubbles could be observed, and an enhanced ultrasound image could also be detected by the acoustic measuring system. Moreover, the mean grayscale of images presented a good linear correlation to the H_2O_2 concentrations within the range of $0–250 \times 10^{-6}$ M. Therefore, this strategy could be used to diagnose ROS-related pathological disease with an excellent sensitivity and resolution. In another work, Peng et al. demonstrated that the oxygen produced by PBNPs could increase the ratio of oxygenated hemoglobin and deoxygenate hemoglobin of the tumor tissue, and then enhance the signal intensity of T_2-weighted imaging.[93]

To further promote the application of PBNPs in disease theranostics, it is essential to prepare PBNPs with higher nanoenzyme activity. For this consideration, the catalytic mechanism and influence factors of nanoenzyme activity require further exploration, such as particle size, morphology, and surface properties.

8. The Key to Clinical Translation

PB, approved by FDA, for internal radioactive contamination in the event of a nuclear attack or a "dirty bomb" is thermodynamically stable and presents excellent biocompatibility.[58] Though long-term moisture loss can lead to a physiochemical change and compromise product quality, PB still meets the FDA specification of >150 mg g^{-1} for cesium[94] and >250 mg g^{-1} for thallium[95] after about 10 years of long-term storage, suggesting the good storage stability of PB. It is undeniable that PBNPs possess unusual properties and have enormous potentials in the exploration of nanotheranostic venues. Having comprehensively reviewed the reported studies on PBNPs, the evaluation tests were just performed in simple laboratory testing, which should be further evaluated in real biological systems, living animals, and in human beings. Therefore, the clinical translation of such nanomaterials is of great challenge at present.

The development process from drug discovery toward commercial products is divided into five stages (**Figure 7**). The phase from preclinical in vitro studies to clinical trials is a critical period in the final approval of nanomedicines. Extensive researches on the clinical applications of nanomedicines indicate that most of the late-stage clinical failures can be attributed to lack of efficacy, toxicity issues, or less than optimal absorption, distribution, metabolism and elimination (ADME).[96] As far as clinical nanotheranostic is concerned, the intrinsic quality, pharmacokinetics and safety of PBNPs should be systematically evaluated for clinical translation.[97]

8.1. The Quality of Nanotheranostic Platforms

There are no systematic investigations on the size-, composition- and shape-dependent photothermal, photoacoustic, and MRI-related properties of PBNPs. For example, the relaxation values are very sensitive to the size and shape of nanoparticles, which are important for MRI contrast.[98] Moreover, it is highly desired to improve the biological potency of PBNPs to provide precise, complementary, and reliable information regarding the lesion, and excellent therapeutic efficacy for synergistic treatment.

A significant feature for nanomedicine in clinical trial or appeared on the market is the simple formulations which make them easy to be controlled and prepared. Paradoxically, PBNPs are designed and constructed wheels within wheels
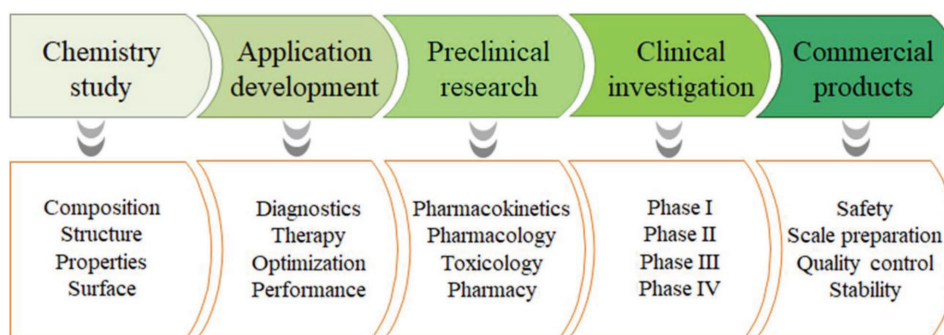

Figure 7. The five phases of nanomedicine development culminating in commercial products.

**ADVANCED
SCIENCE NEWS**
www.advancedsciencenews.com

**ADVANCED
HEALTHCARE
MATERIALS**
www.advhealthmat.de

with complicated formulations to fulfill multifunctions, which make it difficult for scale-up production. The complex production parameters of nanotheranostic such as industrial scale-up validation, manufacturing process, quality control, and batch-to-batch reproducibility, impede the clinical applications of such nanomedicine.[99] In addition, product analysis and reproducibility are also key obstacles to produce good manufacturing practice (GMP)-compliant nanomedicines. Finally, the lack of a clear regulatory framework to approve new nanotheranostic products is also an obstacle for clinical translation of PBNPs. Regulations and standardized methods are significant for defining concept, characterization, quality control, clinical trials, and approval process of novel nanotheranostic products, which still have a long way to go.

8.2. Pharmacokinetics

Though significant progress has been made in the past decade, PBNPs are far from reaching the expectations. Ideally, once delivered in the body, the nanoparticles should overcome a series of biological obstacles including interactions with blood pool, poor penetration, and inefficient cellular uptake,[100] perform desired functions and exit from the body without any deleterious effect. It is necessary for clinical application to investigate the biological behavior of PBNPs and establish their imaging and therapeutic efficiency in the living organisms. In vivo disposition of nanoparticles is the consequence of a complex combination, which is related to their formulation, morphology, size and surface properties.

To date, a few studies have reported in vivo data after intravenous administrate of the nanoparticles, which present a rapid tumor accumulation via enhanced permeability and retention (EPR) effect for large nanoparticles[88] and a long blood circulation time of 45–60 min for small ones.[101] Few researchers focus on nanoparticles excretion. As far as we know, PBNPs were eliminated via urine and faece pathways after oral administration[102] and via glomerular clearing for ultrasmall nanoparticles after intravenous route.[103]

8.3. Safety

Numerous reports have revealed that safety and toxicity issues affect a wide variety of nanoparticles,[104] which likely restrict many new nanomedicines from being approved for clinical trials by the administrator. Therefore, it is essential to comprehensively assess the toxicity of any nanoparticles in preclinical models before clinical trial or administration in human body. Chen et al. investigated the long-term toxicity of PBNPs after short exposure. The results demonstrated that PBNPs presented little influence on mice survival, some acute toxicity, and very low long-term toxicity after short exposure, indicating that the PBNPs are relatively safe.[105] It was reported that citrate-coated PBNPs also showed no detectable cytotoxicity.[69] Thus, it is essential to thoroughly investigate the safety of PBNPs with respect to their particular clinical application.

Ligands are usually utilized to modify PBNPs to endow them with features of improved water solubility, excellent biocompatibility,

prolonged blood circulation, and glomerular clearing. Moreover, specific targeting moiety and environmental stimuli (such as pH, redox potential, enzymes, temperature, and photo) can also be conjugated to the nanotheranostic to facilitate efficient and spatiotemporal controlled delivery and release of the theranostic agents at the target sites,[106] thus fulfilling the requirements of maximum theranostic efficacy and minimum toxicity. The roles of decorated materials for PBNPs need to be investigated thoroughly including the pharmacokinetics, biodistribution, acute, and long-term toxicity. All these assays are the requirements for regulatory evaluation and approval from government and the market. Hence, there are still many obstacles to overcome regarding the translation of nanotheranostic into clinic.

9. Summary and Outlook

As summarized in this chapter, PBNPs have been employed as a promising theranostic agent in the field of biomedical. The nanoparticles possess some unique properties of easy to synthesis, favorable biocompatibility, biomedical imaging (such as photoacoustic imaging and magnetic resonance imaging) or as a drug carrier to achieve synergetic therapy. Compared with commercial contrast agents, PBNPs are a powerful competitor as theranostic agent. Moreover, PBNPs can decontaminate Cs^+ and Tl^+ by promoting the elimination rates in vivo. With nanoenzyme activities, PBNPs have been investigated in the terms of eliminating inflammation and regulating oxygen partial pressure of the tumor tissue. The multifunctional nanotheranostic platform can be developed through fine-tuning of the dopant, size, morphology, and surface modifications of PBNPs. Even so, all these studies are still in the prototype stage for the development of PBNPs as a clinically available nanotherapeutic agent.

Although a number of researches have been conducted in the aspect of synthesis, surface modification and the regulation of nanoparticle's size and morphology, the influence factors of PBNPs for diagnosis and treatment effect are still not investigated systematically. For example, the crystallization extent, size, shape, the type and quantity of surface modification materials to improve contrast image, photothermal properties, adsorption of Cs^+ and Tl^+, and the nanoenzyme catalysis activities are still necessary to research. For this purpose, the relevant mechanisms need to be further clarified including the nanoenzyme catalysis behavior. In order to obtain high-quality PBNPs with higher theranostic efficacy, it is essential to carry out the mechanism studies. We should also pay more attention to the formation mechanism of PBNPs in the future, which is helpful to precisely regulate the properties of PBNPs. The prolonged blood circulation time and targeted delivery of PBNPs are another promising directions. The enrichment of nanotheranostic agents at the desired biological site can achieve better therapeutic effect at a lower dosage.

On the other hand, the biological behavior of PBNPs is still not fully understood after intravenous injection. For instance, the relationship between surface modification, size, morphology, and the blood circulation time, sites of metabolism, excretion pathway needs to be revealed urgently. Besides, the development of evaluation model that can realistically and

consistently simulate complexity of the in vivo environment in humans will be attractive in the future. Furthermore, the pharmacokinetics characteristics and biosafety evaluation of PBNPs are necessary to be further explored for their potential clinical translation.

With the continuous deepening research on the synthesis process, formation mechanism, and biological behavior, higher performance of PBNPs can be obtained. This will effectively promote the clinical translation of PBNPs as multifunctional theranostic agents.

Conflict of Interest

The authors declare no conflict of interest.

[1] M. Shatruk, A. Dragulescu-Andrasi, K. E. Chambers, S. A. Stoian, E. L. Bominaar, C. Achim, K. R. Dunbar, *J. Am. Chem. Soc.* **2007**, *129*, 6104.

[2] B. Kong, J. Tang, C. Selomulya, W. Li, J. Wei, Y. Fang, Y. C. Wang, G. F. Zheng, D. Zhao, *J. Am. Chem. Soc.* **2014**, *136*, 6822.

[3] a) J. F. Keggin, F. D. Miles, *Nature* **1936**, *137*, 577; b) F. Herren, P. Fischer, A. Ludi, W. Halg, *Inorg. Chem.* **1980**, *19*, 956.

[4] B. Kong, C. Selomulya, G. Zheng, D. Zhao, *Chem. Soc. Rev.* **2015**, *44*, 7997.

[5] H. J. Buser, D. Schwarzenbach, W. Petter, A. Ludi, *Inorg. Chem.* **1977**, *16*, 2704.

[6] J. K. Zareba, J. Szeremeta, M. Waszkielewicz, M. Nyk, M. Samoć, *Inorg. Chem.* **2016**, *55*, 9501.

[7] M. B. Zakaria, T. Chikyow, *Coord. Chem. Rev.* **2017**, *352*, 328.

[8] a) A. Takahashi, H. Tanaka, D. Parajuli, T. Nakamura, K. Minami, Y. Sugiyama, Y. Hakuta, S. Ohkoshi, T. Kawamoto, *J. Am. Chem. Soc.* **2016**, *138*, 6376; b) M. P. Suh, H. J. Park, T. K. Prasad, D. Lim, *Chem. Rev.* **2012**, *112*, 782; c) X. Li, Y. Liu, C. Zhang, T. Wen, L. Zhuang, X. Wang, G. Song, D. Chen, Y. Ai, T. Hayat, X. Wang, *Chem. Eng. J.* **2018**, *336*, 241; d) Y. F. Guo, Q. C. Fang, J. Xu, F. X. Bu, W. Zhang, M. Hu, J. S. Jiang, *J. Nanosci. Nanotechnol.* **2018**, *18*, 3059.

[9] a) L. Wang, Y. Han, X. Feng, J. Zhou, P. Qi, B. Wang, *Coord. Chem. Rev.* **2016**, *307*, 361; b) C. Zhang, Y. Xu, M. Zhou, L. Liang, H. Dong,

[10] F. S. Hegner, J. R. Galán-Mascarós, N. López, *Inorg. Chem.* **2016**, *55*, 12851.

[11] P. Ni, Y. Sun, H. Dai, W. Lu, S. Jiang, Y. Wang, Z. Li, Z. Li, *Sens. Actuators, B* **2017**, *240*, 1314.

[12] Y. Zhang, B. Huang, F. Yu, Q. Yuan, M. Gu, J. Ji, Y. Zhang, Y. Li, *Microchim. Acta* **2018**, *185*, 86.

[13] a) N. Grimaldi, F. Andrade, N. Segovia, L. Ferrer-Tasies, S. Sala, J. Veciana, N. Ventosa, *Chem. Soc. Rev.* **2016**, *45*, 6520; b) M. Molina, M. Asadian-Birjand, J. Balach, J. Bergueiro, E. Miceliac, M. Calderon, *Chem. Soc. Rev.* **2015**, *44*, 6161; c) V. Gutierrez, A. B. Seabra, R. M. Reguera, J. Khandared, M. Calderon, *Chem. Soc. Rev.* **2016**, *45*, 152; d) Y. Liu, M. Li, F. Yang, N. Gu, *Sci. China Mater.* **2017**, *60*, 471; e) Z. L. Chai, X. F. Hu, W. Y. Lu, *Sci. China Mater.* **2017**, *60*, 504.

[14] T. T. Shang, J. X. Liu, Y. Chen, Z. C. Hu, L. M. Deng, H. T. Ran, P. Li, Y. Y. Zheng, D. Wang, Z. G. Wang, Y. Sun, *Part. Part. Syst. Charact.* **2018**, *35*, 1700306.

[15] a) F. X. Bu, C. J. Du, Q. H. Zhang, J. S. Jiang, *CrystEngComm* **2014**, *16*, 3113; b) L. Catala, T. Mallah, *Coord. Chem. Rev.* **2017**, *346*, 32; c) A. Indra, U. Paik, T. Song, *Angew. Chem., Int. Ed.* **2018**, *57*, 1241.

[16] a) M. Hu, J. S. Jiang, R. P. Jia, Y. Zeng, *CrystEngComm* **2009**, *11*, 2257; b) B. Kong, J. Tang, Z. Wu, J. Wei, H. Wu, Y. Wang, G. Zheng, D. Zhao, *Angew. Chem., Int. Ed.* **2014**, *53*, 2888; c) K. E. Funck, M. G. Hilfiger, C. P. Berlinguette, M. Shatruk, W. Wernsdorfer, K. R. Dunbar, *Inorg. Chem.* **2009**, *48*, 3438.

[17] T. Uemura, S. Kitagawa, *J. Am. Chem. Soc.* **2003**, *125*, 7814.

[18] a) Z. Qian, Z. Liang, J. Li, *Electrochim. Acta* **2008**, *53*, 3050; b) J. Zhai, Y. Zhai, L. Wang, S. Dong, *Inorg. Chem.* **2008**, *47*, 7071; c) T. Uemura, A. Masaaki Ohba, S. Kitagawa, *Inorg. Chem.* **2004**, *43*, 7339.

[19] R. Yang, Z. B. Qian, J. Q. Deng, *J. Electrochem. Soc.* **1998**, *145*, 2231.

[20] Z. Q. Jia, G. B. Sun, *Colloids Surf., A* **2007**, *302*, 326.

[21] M. Hu, J. S. Jiang, Y. Zeng, *Chem. Commun.* **2010**, *46*, 1133.

[22] M. Hu, N. L. K. Torad, Y. D. Chiang, K. C. W. Wu, Y. Yamauchi, *CrystEngComm* **2012**, *14*, 3387.

[23] X. P. Shen, S. K. Wu, Y. Liu, K. Wang, Z. Xu, W. Liu, *J. Colloid Interface Sci.* **2009**, *329*, 188.

[24] Y. Ding, Y. L. Hu, G. Gu, X. H. Xia, *J. Phys. Chem. C* **2009**, *113*, 14838.

[25] X. L. Zhang, C. H. Sui, J. Gong, R. Yang, Y. Q. Luo, L. Y. Qu, *Appl. Surf. Sci.* **2007**, *253*, 9030.

[26] L. Qian, R. Zheng, L. T. Zheng, *J. Nanopart. Res.* **2013**, *15*, 1806.

[27] M. Hu, S. Furukawa, R. Ohtani, H. Sukegawa, Y. Nemoto, J. Reboul, S. Kitagawa, Y. Yamauchi, *Angew. Chem., Int. Ed.* **2012**, *51*, 984.

[28] M. Hu, A. A. Belik, M. Imura, Y. Yamauchi, *J. Am. Chem. Soc.* **2013**, *135*, 384.

[29] S. H. Lee, Y. D. Huh, *Bull. Korean Chem. Soc.* **2012**, *33*, 1078.

[30] R. McHale, N. Ghasdian, Y. Liu, M. B. Ward, N. S. Hondo, H. Wang, Y. Miao, R. Brydson, X. Wang, *Chem. Commun.* **2010**, *46*, 4574.

[31] S. Vaucher, M. Li, S. Mann, *Angew. Chem., Int. Ed.* **2000**, *39*, 1793.

[32] G. Liang, J. Xu, X. Wang, *J. Am. Chem. Soc.* **2009**, *131*, 5378.

[33] l. E. A. De, M. Verwegen, F. D. Sikkema, M. Comellas-Aragones, A. Kirilyuk, T. Rasing, R. J. Nolte, J. J. Cornelissen, *Chem. Commun.* **2008**, *13*, 1542.

[34] a) H. Alamri, N. Ballot, J. Long, Y. Guari, J. Larionova, K. Kleinke, H. Kleinke, E. Prouzet, *Chem. Mater.* **2014**, *26*, 875; b) J. M. Domínguez-Vera, E. Colacio, *Inorg. Chem.* **2003**, *42*, 6983; c) A. Johansson, E. Widenkvist, J. Lu, M. Boman, U. Jansson, *Nano Lett.* **2005**, *5*, 1603.

[35] X. L. Wu, M. H. Cao, C. W. Hu, X. Y. He, *Cryst. Growth Des.* **2006**, *6*, 26.

[36] B. Chen, J. F. Sun, F. G. Fan, X. Z. Zhang, Z. G. Qin, P. Wang, Y. Li, X. Q. Zhang, F. Liu, Y. L. Liu, M. Ji, N. Gu, *Nanoscale* **2018**, *10*, 7369.

[37] a) X. D. Li, X. L. Liang, F. Ma, L. J. Jing, L. Lin, Y. B. Yang, S. S. Feng, G. L. Fu, X. L. Yue, Z. F. Dai, *Colloids Surf., B* **2014**, *123*, 629; b) D. Wang, J. Zhou, R. Chen, R. Shi, G. Zhao, G. Xia, R. Li, Z. Liu, J. Tian, H. Wang, Z. Guo, H. Wang, Q. Chen, *Biomaterials* **2016**, *100*, 27.

[38] H. Chen, Y. Ma, X. Wang, Z. Zha, *J. Mater. Chem. B* **2017**, *5*, 7051.

[39] H. Y. Lian, M. Hu, C. H. Liu, Y. Yamauchi, K. C. W. Wu, *Chem. Commun.* **2012**, *48*, 5151.

[40] L. Jing, S. Shao, Y. Wang, Y. Yang, X. Yue, Z. Dai, *Theranostics* **2016**, *6*, 40.

[41] P. Zhang, F. Sun, S. Liu, S. Jiang, *J. Controlled Release* **2016**, *244*, 184.

[42] W. Chen, K. Zeng, H. Liu, J. Ouyang, L. Wang, Y. Liu, H. Wang, L. Deng, Y. Liu, *Adv. Funct. Mater.* **2017**, *27*, 1605795.

[43] H. Chen, Y. Ma, X. Wang, X. Wu, Z. Zha, *RSC Adv.* **2017**, *7*, 248.

[44] P. Xue, K. K. Y. Cheong, Y. Wu, Y. Kang, *Colloids Surf., B* **2015**, *125*, 277.

[45] Y. Y. Su, Z. Teng, H. Yao, S. J. Wang, Y. Tian, Y. L. Zhang, W. F. Liu, W. Tian, L. J. Zheng, N. Lu, Q. Q. Ni, X. D. Su, Y. X. Tang, J. Sun, Y. Liu, J. Wu, G. F. Yang, G. M. Lu, L. J. Zhang, *ACS Appl. Mater. Interfaces* **2016**, *8*, 17038.

[46] D. Wang, J. Zhou, R. Shi, H. Wu, R. Chen, B. Duan, G. Xia, P. Xu, H. Wang, S. Zhou, C. Wang, H. Wang, Z. Guo, Q. Chen, *Theranostics* **2017**, *7*, 4605.

[47] J. Peng, Q. Yang, W. Li, L. Tan, Y. Xiao, L. Chen, Y. Hao, Z. Qian, *ACS Appl. Mater. Interfaces* **2017**, *9*, 44410.

[48] J. Panyam, V. Labhasetwar, *Adv. Drug Delivery Rev.* **2012**, *64*, 61.

[49] S. J. Wang, C. S. Chen, L. C. Chen, *Sci. Technol. Adv. Mater.* **2013**, *14*, 044405.

[50] X. Li, X. Yue, J. Wang, X. Liang, L. Jing, L. Lin, Y. Yang, S. Feng, Y. Qian, Z. Dai, *Sci. Bull.* **2016**, *61*, 148.

[51] J. Qian, S. Cai, S. Yang, D. Hua, *J. Mater. Chem. A* **2017**, *5*, 22380.

[52] M. Ishizaki, S. Akiba, A. Ohtani, Y. Hoshi, K. Ono, M. Matsuba, T. Togashi, K. Kananizuka, M. Sakamotoa, A. Takahashi, T. Kawamoto, H. Tanaka, M. Watanabe, M. Arisaka, T. Nankawa, M. Kurihar, *Dalton Trans.* **2013**, *42*, 16049.

[53] H. Fujita, H. Sasano, R. Miyajima, A. Sakoda, *Adsorption* **2014**, *20*, 905.

[54] H. Fujita, R. Miyajima, A. Sakoda, *Adsorption* **2015**, *21*, 195.

[55] C. Lavaud, M. Kajdan, E. Compte, J. C. Maurel, J. L. K. Him, P. Bron, E. Oliviero, J. Long, J. Larionova, Y. Guari, *New J. Chem.* **2017**, *41*, 2887.

[56] T. Koshiyama, M. Tanaka, M. Honjo, Y. Fukunaga, T. Okamura, M. Ohba, *Langmuir* **2018**, *34*, 1666.

[57] J. Qian, J. Xu, L. Kuang, D. Hua, *ChemPlusChem* **2017**, *82*, 888.

[58] N. Sandal, G. Mittal, A. Bhatnagar, D. P. Pathak, A. K. Singh, *J. Drug Delivery* **2017**, *2017*, 4875784.

[59] a) J. N. Liu, W. B. Bu, J. L. Shi, *Chem. Rev.* **2017**, *117*, 6160; b) J. Zhou, G. Tian, L. Zeng, X. Song, X. W. Bian, *Adv. Healthcare Mater.* **2018**, *3*, 1800022; c) J. Mou, Y. Chen, M. Ma, K. Zhang, C. Wei, H. Chen, J. Shi, *Sci. China Mater.* **2015**, *58*, 294.

[60] N. Q. Bui, S. W. Cho, M. S. Moorthy, S. M. Park, Z. Piao, S. Y. Nam, H. W. Kang, C. S. Kim, J. Oh, *Sci. Rep.* **2018**, *8*, 2000.

[61] a) D. L. Longo, R. Stefania, C. Callari, F. De Rose, R. Rolle, L. Conti, F. Arena, S. Aime, *Adv. Healthcare Mater.* **2017**, *6*, 1600550; b) V. Ntziachristos, D. Razansky, *Chem. Rev.* **2010**, *110*, 2783.

[62] X. Liang, Z. Deng, L. Jing, X. Li, Z. Dai, C. Li, M. Huang, *Chem. Commun.* **2013**, *49*, 11029.

[63] L. Jing, X. Liang, Z. Deng, S. Feng, X. Li, M. Huang, C. Li, Z. Dai, *Biomaterials* **2014**, *35*, 5814.

[64] T. Kim, J. E. Lemaster, F. Chen, J. Li, J. V. Jokerst, *ACS Nano* **2017**, *11*, 9022.

[65] W. Li, R. Chen, J. Lv, H. Wang, Y. Liu, Y. Peng, Z. Qian, G. Fu, L. Nie, *Adv. Sci.* **2018**, *5*, 1700277.

[66] X. Cai, W. Gao, L. Zhang, M. Ma, T. Liu, W. Du, Y. Zeng, H. Chen, J. Shi, *ACS Nano* **2016**, *10*, 11115.

[67] a) J. Mosayebi, M. Kiyasatfar, S. Laurent, *Adv. Healthcare Mater.* **2017**, *6*, 1700306; b) D. Ni, W. Bu, E. B. Ehlerding, W. Cai, J. Shi, *Chem. Soc. Rev.* **2017**, *46*, 7438.

[68] M. Shokouhimehr, E. S. Soehnlen, J. Hao, M. Griswold, C. Flask, X. Fan, J. P. Basilion, S. Basu, S. D. Huang, *J. Mater. Chem.* **2009**, *20*, 5251.

[69] M. Shokouhimehr, E. S. Soehnlen, A. Khitrin, S. Basu, S. D. Huang, *Inorg. Chem. Commun.* **2010**, *13*, 58.

[70] Y. Liu, Q. Guo, X. Zhu, W. Feng, L. Wang, L. Ma, G. Zhang, J. Zhou, F. Li, *Adv. Funct. Mater.* **2016**, *26*, 5120.

[71] X. Cai, W. Gao, M. Ma, M. Wu, L. Zhang, Y. Zheng, H. Chen, J. Shi, *Adv. Mater.* **2015**, *27*, 6382.

[72] M. F. Dumont, H. A. Hoffman, P. R. S. Yoon, L. S. Conklin, S. R. Saha, J. Paglione, R. W. Sze, R. Fernandes, *Bioconjugate Chem.* **2014**, *25*, 129.

[73] N. Lee, D. Yoo, D. Ling, M. H. Cho, T. Hyeon, J. Cheon, *Chem. Rev.* **2015**, *115*, 10637.

[74] L. Cheng, H. Gong, W. Zhu, J. Liu, X. Wang, G. Liu, Z. Liu, *Biomaterials* **2014**, *35*, 9844.

[75] W. Tian, Y. Su, Y. Tian, S. Wang, X. Su, Y. Liu, Y. Zhang, Y. Tang, Q. Ni, W. Liu, M. Dang, C. Wang, J. Zhang, Z. Teng, G. Lu, *Adv. Sci.* **2017**, *4*, 1600356.

[76] N. Zhang, X. Cai, W. Gao, R. Wang, C. Xu, Y. Yao, L. Hao, D. Sheng, H. Chen, Z. Wang, Y. Zheng, *Theranostics* **2016**, *6*, 404.

[77] J. Li, F. Zhang, Z. Hu, W. Song, G. Li, G. Liang, J. Zhou, K. Li, Y. Cao, Z. Luo, K. Cai, *Adv. Healthcare Mater.* **2017**, *6*, 1700005.

[78] Y. Yang, L. Jing, X. Li, L. Lin, X. Yue, Z. Dai, *Theranostics* **2017**, *7*, 466.

[79] Y. Dou, X. Li, W. Yang, Y. Guo, M. Wu, Y. Liu, X. Li, X. Zhang, J. Chang, *ACS Appl. Mater. Interfaces* **2017**, *9*, 1263.

[80] X. Peng, R. Wang, T. Wang, W. Yang, H. Wang, W. Gu, L. Ye, *ACS Appl. Mater. Interfaces* **2018**, *10*, 1084.

[81] G. Fu, W. Liu, S. Feng, X. Yue, *Chem. Commun.* **2012**, *48*, 11567.

[82] a) D. de Melo-Diogo, C. Pais-Silva, D. R. Dias, A. F. Moreira, I. J. Correia, *Adv. Healthcare Mater.* **2017**, *6*, 1700073; b) L. M. A. Ali, E. Mathlouthi, M. Kajdan, M. Daurat, J. Long, R. Sidi-Boulenouar, M. Cardoso, C. Goze-Bac, N. Amdouni, Y. Guari, J. Larionova, M. Gary-Bobo, *Photodiagn. Photodyn. Ther.* **2018**, *22*, 65; c) X. Zhang, L. Y. Xia, X. Chen, Z. Chen, F. G. Wu, *Sci. China Mater.* **2017**, *60*, 487.

[83] W. Zhu, K. Liu, X. Sun, X. Wang, Y. Li, L. Cheng, Z. Liu, *ACS Appl. Mater. Interfaces* **2015**, *7*, 11575.

[84] Z. Li, Y. Zeng, D. Zhang, M. Wu, L. Wu, A. Huang, H. Yang, X. Liu, J. Liu, *J. Mater. Chem. B* **2014**, *2*, 3686.

[85] H. Maaoui, R. Jijie, G. H. Pan, D. Drider, D. Caly, J. Bouckaert, N. Dumitrascuc, R. Chtouroug, S. Szunerits, R. Boukherroub, *J. Colloid Interface Sci.* **2016**, *480*, 63.

[86] B. R. Smith, S. S. Gambhir, *Chem. Rev.* **2017**, *117*, 901.

[87] X. Jia, X. Cai, Y. Chen, S. Wang, H. Xu, K. Zhang, M. Ma, H. Wu, J. Shi, H. Chen, *ACS Appl. Mater. Interfaces* **2015**, *7*, 4579.

[88] X. Cai, X. Jia, W. Gao, K. Zhang, M. Ma, S. Wang, Y. Zheng, J. Shi, H. Chen, *Adv. Funct. Mater.* **2015**, *25*, 2520.

[89] M. Vázquez-González, R. M. Torrente-Rodríguez, A. Kozell, W. C. Liao, A. Cecconello, S. Campuzano, J. M. Pingarrón, I. Willner, *Nano Lett.* **2017**, *17*, 4958.

[90] W. Zhang, S. Hu, J. J. Yin, W. He, W. Lu, M. Ma, N. Gu, Y. Zhang, *J. Am. Chem. Soc.* **2016**, *138*, 5860.

[91] J. Zhou, M. Li, Y. Hou, Z. Luo, Q. Chen, H. Cao, R. Huo, C. Xue, L. Sutrisno, L. Hao, Y. Cao, H. Ran, L. Lu, K. Li, K. Cai, *ACS Nano* **2018**, *12*, 2858.

[92] F. Yang, S. Hu, Y. Zhang, X. Cai, Y. Huang, F. Wang, S. Wen, G. Teng, N. Gu, *Adv. Mater.* **2012**, *24*, 5205.

[93] J. Peng, M. Dong, B. Ran, W. Li, Y. Hao, Q. Yang, L. Tan, K. Shi, Z. Qian, *ACS Appl. Mater. Interfaces* **2017**, *9*, 13875.

[94] A. Mohammad, Y. Yang, M. A. Khan, P. J. Faustino, *J. Pharm. Biomed. Anal.* **2015**, *103*, 85.

[95] A. Mohammad, P. J. Faustino, M. A. Khan, Y. Yang, *Int. J. Pharm.* **2014**, *477*, 122.

[96] a) M. Karimi, A. Ghasemi, P. S. Zangabad, R. Rahighi, S. M. M. Basri, H. Mirshekari, M. Amiri, Z. S. Pishabad, A. Aslani, M. Bozorgomid, D. Ghosh, A. Beyzavi, A. Vaseghi, A. R. Aref, L. Haghani, S. Bahrami, M. R. Hamblin, *Chem. Soc. Rev.* **2016**, *45*, 1457; b) M. A. Dobrovolskaia, *J. Controlled Release* **2015**, *220*, 571; c) Y. Min, J. M. Caster, M. J. Eblan, A. Z. Wang, *Chem. Rev.* **2015**, *115*, 11147.

[97] C. R. Patra, *Nanomedicine* **2016**, *11*, 569.

[98] J. Long, Y. Guari, C. Guérin, J. Larionova, *Dalton Trans.* **2016**, *45*, 17581.

[99] D. Liu, F. Yang, F. Xiong, N. Gu, *Theranostics* **2016**, *6*, 1306.

[100] C. Deng, Y. Jiang, R. Cheng, F. Meng, Z. Zhong, *Nano Today* **2012**, *7*, 467.

[101] M. Perrier, A. Gallud, A. Ayadi, S. Kennouche, C. Porredon, M. Gary-Bobo, J. Larionova, C. Goze-Bac, M. Zanca, M. Garcia, I. Basile, J. Long, J. de Lapuente, M. Borras, Y. Guari, *Nanoscale* **2015**, *7*, 11899.

[102] C. Timchalk, J. A. Creim, V. Sukwarotwat, R. Wiacek, R. S. Addleman, G. E. Fryxell, W. Yantasee, *Health Phys.* **2010**, *99*, 420.

[103] M. Perrier, M. Busson, G. Massasso, J. Long, V. Boudousq, J. P. Pouget, S. Peyrottes, C. Perigaud, C. Porredon-Guarch, J. de Lapuente, M. Borras, J. Larionova, Y. Guari, *Nanoscale* **2014**, *6*, 13425.

[104] a) N. Golbamaki, B. Rasulev, A. Cassano, R. L. M. Robinson, E. Benfenati, J. Leszczynski, M. T. Cronin, *Nanoscale* **2015**, *7*, 2154; b) S. Wuttke, A. Zimpel, T. Bein, S. Braig, K. Stoiber, A. Vollmar, D. Müller, K. Haastert-Talini, J. Schaeske, M. Stiesch, G. Zahn, A. Mohmeyer, P. Behrens, O. Eickelberg, D. A. Bölükbas, S. Meiners, *Adv. Healthcare Mater.* **2017**, *6*, 1600818.

[105] Y. Chen, L. Wu, Q. Wang, M. Wu, B. Xu, X. Liu, J. Liu, *Hum. Exp. Toxicol.* **2016**, *35*, 1123.

[106] Y. Ma, J. Huang, S. Song, H. Chen, Z. Zhang, *Small* **2016**, *12*, 4936.